



This is the accepted manuscript made available via CHORUS. The article has been published as:

Heterogeneous message passing for heterogeneous networks

George T. Cantwell, Alec Kirkley, and Filippo Radicchi

Phys. Rev. E **108**, 034310 — Published 26 September 2023

DOI: [10.1103/PhysRevE.108.034310](https://doi.org/10.1103/PhysRevE.108.034310)

Heterogeneous message passing for heterogeneous networks

George T. Cantwell,¹ Alec Kirkley,^{2,3,4} and Filippo Radicchi⁵

¹*Santa Fe Institute, 1399 Hyde Park Road, Santa Fe, New Mexico 87501, USA*

²*Institute of Data Science, University of Hong Kong, Hong Kong*

³*Department of Urban Planning and Design, University of Hong Kong, Hong Kong*

⁴*Urban Systems Institute, University of Hong Kong, Hong Kong*

⁵*Center for Complex Networks and Systems Research,*

School of Informatics, Computing, and Engineering,

Indiana University, Bloomington, Indiana 47408, USA

Message passing (MP) is a computational technique used to find approximate solutions to a variety of problems defined on networks. MP approximations are generally accurate in locally tree-like networks but require corrections to maintain their accuracy level in networks rich with short cycles. However, MP may already be computationally challenging on very large networks and additional costs incurred by correcting for cycles could be prohibitive. We show how the issue can be addressed. By allowing each node in the network to have its own level of approximation, one can focus on improving the accuracy of MP approaches in a targeted manner. We perform a systematic analysis of 109 real-world networks and show that our node-based MP approximation is able to increase both the accuracy and speed of traditional MP approaches. We find that, compared to conventional MP, a heterogeneous approach based on a simple heuristic is more accurate in 81% of tested networks, faster in 64% of cases, and both more accurate and faster in 49% of cases.

I. INTRODUCTION

Message passing (MP), sometimes called belief propagation or the cavity method, is a computational technique aimed at solving problems or characterizing processes on networks [1]. Examples include spreading processes [2–7], community detection [8, 9], sampling strategies [10], spectral properties [11, 12], and percolation [13–17].

MP techniques are closely related to mean-field approximations [18, 19], in which one relates a quantity of interest at each node to those of their neighbors. For example, the event in which someone catches an infectious disease is related to whether the people they are in contact with catch the disease. A mean-field analysis proceeds by replacing unknown quantities defined on the nodes of the network with average or expected values, (incorrectly!) assuming that these quantities are independent. One derives a set of self-consistent equations to be solved. In such mean-field approximations there is one equation for each node in the network. Unfortunately, these approximations can be inaccurate.

MP approaches follow a similar logic but at least partially account for correlations induced by edges. In place of the independence assumption of a mean-field approximation, one makes a *conditional* independence assumption. As for mean-field approximations, MP approximations introduce a system of self-consistent equations to be solved. Now, however, there are two equations for each *edge* in the network.

Conventional MP techniques are often exact on trees (networks without cycles), and are justified on general networks by a locally tree-like assumption. When applied to real networks, MP methods often generate fairly accurate predictions [20]. Mistakes in the predictions can be attributed to the inability of the locally tree-like as-

sumptions to account for the correlations introduced by cycles.

However, because many networks have a relatively high density of short cycles it is important to be able to account for them. Social networks, for instance, typically have large numbers of triangles [21, 22]. One mechanism that would give rise to a large number of triangles is triadic closure—the process whereby two of your friends become friends with each other. Likewise shared familial, vocational, or geographical ties can lead to densely connected subgroups of individuals, and hence large numbers of triangles.

A few attempts to account for correlations due to short loops exist in the literature. Some previous methods, such as those of Refs. [23, 24], do not generalize to arbitrary combinations of short loops, or suffer from the limitation of being problem specific. One promising direction is the approach of Cantwell and Newman [25], which accounts for correlations caused by arbitrary short loops.

The framework of Ref. [25] relies on a procedure for constructing appropriately defined neighborhoods around each node. We will refer to this procedure as the neighborhood message passing (NMP) approach. The size of the neighborhoods can be increased in order to improve the accuracy of the predictions, but this increase in accuracy comes at the cost of an increasingly complex set of equations to solve. The utility of NMP follows from the fact that the method provides good results for relatively small neighborhoods. The accuracy of NMP has been demonstrated for bond percolation, spectral properties of sparse matrices, and the Ising model [25, 26].

However, many networks have heterogeneous degree distributions [27], and this property may cause unique problems. First, heterogeneous degree distributions can imply a large density of short cycles [28]. In a random

graph with n nodes and degree distribution p_k , the expected number of triangles per node $\langle t \rangle$ is to leading order

$$\langle t \rangle \propto \frac{\langle k^2 \rangle^3}{2n \langle k \rangle^3} \quad (1)$$

where $\langle k \rangle = \sum_k k p_k$ and $\langle k^2 \rangle = \sum_k k^2 p_k$. If $\langle k^2 \rangle$ diverges as $n^{1/3}$ or faster, the expected number of triangles per node diverges, even if the network is sparse.

Second, heterogeneous degree distributions may cause MP schemes to be somewhat more computationally demanding than they are in networks with homogeneous degree distributions. By definition, each node of degree k has k edges. Each of these edges has a corresponding equation that typically depends on $k - 1$ other variables. Evaluating these equations for a network with n nodes may thus require $\mathcal{O}(n \langle k^2 \rangle)$ operations. When $\langle k^2 \rangle$ is large (or diverging) the numerical solution of the equations could be expensive.

Heterogeneous degree distributions may thus cause both accuracy and speed degradation for traditional MP approaches. As discussed, the NMP approach trades off speed for accuracy in networks with short cycles. For networks with relatively homogeneous degree distributions, such as social or biological networks [22], the cost may be quite acceptable. However, NMP may considerably exacerbate the speed issues caused by heterogeneous degree distributions, and the additional cost may simply be prohibitive. In this paper, we present a solution to this problem, allowing for accurate and fast approximations for real-world networks with heterogeneous degree distributions.

Our solution embraces heterogeneity and relies on an appropriately heterogeneous approximation. Large-degree nodes can be approximated by conventional mean-field approximations, since the aggregate fluctuations of their neighbors should be small by the law of large numbers. Conversely, low-degree nodes can be approximated either by conventional MP, or by NMP when there is a large density of short loops. By tailoring the level of approximation for each node we can deploy our methods to arbitrary networks.

The remaining sections of the paper are structured as follows. In Sec. II, we systematically explore the properties of neighborhoods in real-world networks, observing considerable heterogeneity. In Secs. III and IV, we first derive and then test a heterogeneous NMP approach for computing the spectral properties of real networks. We find that our approach is able to increase on both the accuracy and the speed of MP in about 50% of cases. Finally, in Sec. V, we show that the NMP approach can be also used in estimating properties of the zero-field Ising model on networks, and then conclude the paper.

II. NEIGHBORHOOD HETEROGENEITY

In the NMP approach, one sets a value of r for the network. Given $r \geq 0$, one constructs the neighborhoods of

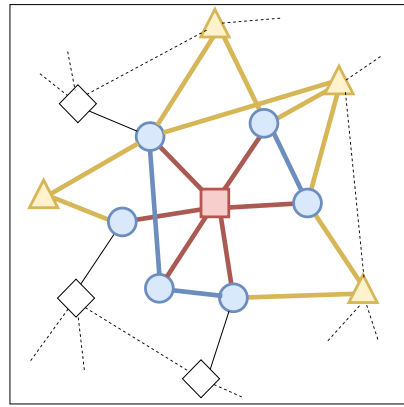


FIG. 1: **Definition of the r -neighborhood of a node.** We denote the order r neighborhood of node i as E_i^r . Neighborhoods are naturally defined in terms of edges; the set of nodes that are in the neighborhood, i.e., N_i^r , is composed of all nodes at the end of at least one edge in E_i^r . For the focal node i , shown as a red square in the figure, the neighborhood E_i^0 consists of all edges incident to the node, depicted in red (edges between the square and the circles). For E_i^1 , the neighborhood consists of all edges in E_i^0 along with all edges between neighbors of i , depicted in blue (edges between circles). For E_i^2 , the neighborhood consists of all edges in E_i^1 along with all edges on paths of length two neighbors of i , depicted in yellow (edges between circles and triangles). Nodes in the neighborhoods N_i^0 and N_i^1 are denoted by blue circles; N_i^2 is composed of all nodes denoted as either blue circles or yellow triangles.

each node, defined by a set of edges. Specifically, the r -neighborhood around node i , denoted E_i^r , consists of all edges incident to node i , along with all paths of length r or shorter between nodes adjacent to i . An example of this construction is shown in Fig. 1. All nodes that appear at the end of edges in E_i^r compose the set N_i^r . **Note, r -neighborhoods are defined by cycles; the neighborhood N_i^r is not equivalent to the set of nodes that are at distance r from node i .**

To begin, we compute the size of the neighborhoods of 109 real-world networks. Percolation properties of these networks have been investigated in Refs. [15, 24, 29]. The corpus contains networks of different nature, including technological, biological, social, and information networks. See Tables I- III for details. All networks in the corpus are relatively sparse. Other structural properties—e.g., size, clustering coefficient, average length, degree distribution and degree correlations—vary greatly within the corpus.

To get a sense of how the NMP approximation will scale, we look at the dependence of the size of the largest neighborhood, i.e., $|N_{\max}^r| = \max_i |N_i^r|$, with the network size. Our results, reported in Fig. 2, indicate that the size of the largest neighborhood grows with the network size. There are a few networks for which the largest neighborhood are very small compared to the network size. This is the case of networks with homogeneous degree distri-

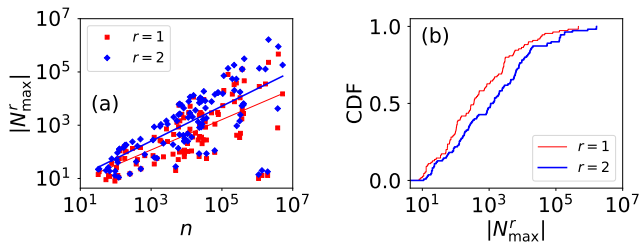


FIG. 2: **Size of the largest neighborhoods in real-world networks.** (a) We consider 109 real-world networks. For each network, we evaluate the size of the largest neighborhood $|N_{\max}^r|$ and plot it as a function of the size n of the network. Each point in the plot refers to a network. The lines are power-law fits of the data points, i.e., $|N_{\max}^r| \sim n^{\beta^r}$. The best fit is obtained using linear regression on the logarithms of the data. We find $\beta^1 = 0.57$ (Pearson's linear correlation coefficient 0.69) and $\beta^2 = 0.67$ (0.71). (b) Cumulative distribution function (CDF) of $|N_{\max}^r|$. Data are the same as in panel (a).

butions and/or strong spatial embedding, as for example road networks. Networks with heterogeneous degree distributions are instead characterized by large neighborhoods. To give quantitative references, we find that for 50% of the networks, $|N_{\max}^2| \geq 0.22n$.

In summary, these results show that some networks contain large neighborhoods. If the NMP equations scale poorly with the neighborhood size then the approach will be infeasible. In the next section, we remedy this by adjusting r at the level of individual nodes.

III. HETEROGENEOUS MESSAGE PASSING

A. General approach

In the NMP approach of [25] one chooses a single value of r . Using the neighborhoods, and specific to the problem at hand, one derives a set of MP equations of the form

$$H_i = \Phi_i(\mathbf{H}_{i \leftarrow N_i^r}) \quad (2)$$

$$H_{i \leftarrow j} = \Phi_{i \leftarrow j}(\mathbf{H}_{i \leftarrow N_j^r \setminus N_i^r}), \quad (3)$$

where $\mathbf{H}_{i \leftarrow N_i^r}$ is the vector of $H_{i \leftarrow j}$ for $j \in N_i^r$, and Φ_i and $\Phi_{i \leftarrow j}$ are problem-specific MP functions. A MP algorithm consists of **initializing the variables (e.g., at random) and then iterating this set of equations until they converge to a fixed point. In general, convergence may not be mathematically guaranteed; necessary and sufficient conditions for convergence are unclear, but this does not appear to be a significant problem in practice [30, 31].** When setting $r = 0$, these equations reduce to the conventional MP ones. Increasing r should increase the accuracy of the approach, but potentially with a considerable increase of the computational cost.

As discussed, in a heterogeneous network there may be competing considerations on how to appropriately set the value of r . For example, in a sparse network with a high density of short cycles, we are likely to require $r \geq 1$ for an accurate approximation. On the other hand, heterogeneous degree distributions may even increase the cost to solving the traditional MP equations. Further increasing the complexity of the equations to be solved by increasing r may simply be untenable. How should one proceed?

Our solution is based on the simple observation that the neighborhood formalism does not actually require that each neighborhood is constructed with the same value of r . Around nodes that are dense with short cycles but have relatively low degree, we can increase r . This increases accuracy with only a small increase to computational cost. Conversely, for nodes with very high degrees, we can decrease r to reduce computational burden without a significant decrease in accuracy. In fact, for nodes with extremely high degree we should find $H_{i \leftarrow j} \approx H_j$, i.e., that the messages have the same numerical value as the marginals. Making this approximation corresponds to a mean-field approximation, and helps to further reduce the computational cost caused by high-degree nodes.

We allow each node i to have its own approximation value r_i . Re-writing the NMP equations but with heterogeneous r we get

$$H_i = \Phi_i(\mathbf{H}_{i \leftarrow N_i^{r_i}}) \quad (4)$$

$$H_{i \leftarrow j} = \begin{cases} H_j & \text{if } r_j = -1 \\ \Phi_{i \leftarrow j}(\mathbf{H}_{i \leftarrow N_j^{r_j} \setminus N_i^{r_i}}) & \text{if } r_j \geq 0. \end{cases} \quad (5)$$

Note we allow $r_j = -1$ and use this notation to indicate the standard mean-field approximation.

Below, we test the ability of heterogeneous NMP to account for the spectral properties of large networks. We find that increasing r does indeed increase the accuracy of the approach over conventional MP, **at the expense of increased compute time. However, by setting $r_i = 0$ for large-degree nodes, we retain much of the improved accuracy for only a small additional cost compared to conventional MP. Remarkably, by setting $r_i = -1$ for the large-degree nodes, we find it is possible to **derive an algorithm that is able to improve on both accuracy and speed, compared to conventional MP.****

B. Spectral density estimation

As a specific application, we consider an heterogeneous NMP approximation for the estimation of the spectral density of the graph operators, e.g., adjacency matrix, graph Laplacian. The spectral density of matrix \mathbf{M} with eigenvalues λ_k is defined

$$\rho(z) = -\frac{1}{n\pi} \sum_{k=1}^n \frac{1}{z - \lambda_k} \quad (6)$$

for complex z .

Following Ref. [25], one can approximate $\rho(z)$ by first solving the MP equations

$$H_i(z) = \sum_{w \in W_i} |w| \prod_{j \in w} \frac{1}{z - H_{i \leftarrow j}(z)} \quad (7)$$

$$H_{i \leftarrow j}(z) = \sum_{w \in W_{j \setminus i}} |w| \prod_{k \in w} \frac{1}{z - H_{j \leftarrow k}(z)}, \quad (8)$$

where the sum is over all closed walks w in the neighborhood N_i^0 or $N_j^0 \setminus N_i^0$ respectively, and $|w|$ is the product of all edges in the walk. These equations can be solved relatively efficiently using matrix algebra—see [25]—and finally one approximates

$$\rho(z) = -\frac{1}{n\pi} \sum_{i=1}^n \frac{1}{z - H_i(z)}. \quad (9)$$

In the NMP heterogeneous approximation, we mostly leave the equations unchanged, except that now we allow the neighborhood $N_i^{r_i}$ of node i to be defined with its own value of r_i , and also allow for the mean-field approximation if $r_i = -1$,

$$H_{i \leftarrow j}(z) = \begin{cases} H_j(z) & r_j = -1 \\ \sum_{w \in W_{j \setminus i}} |w| \prod_{k \in w} \frac{1}{z - H_{j \leftarrow k}(z)} & r_j \geq 0. \end{cases} \quad (10)$$

To establish the desired value of r_i for each node i , we set parameters r_{\min} , r_{\max} , and K . The value of r_i is chosen to be the largest value $r_{\min} \leq r_i \leq r_{\max}$ so that $|N_i^{r_i}| \leq K$. This procedure imposes $r_i = r_{\min}$ whenever the degree of node i is larger than K . Otherwise, it imposes r_i as large as possible so that the neighborhood contains no more than K nodes.

IV. NUMERICAL RESULTS

We estimate the spectral density of the graph Laplacian of the real networks in our corpus. **The spectral properties of the Laplacian are important for many graph applications, including graph invariants (e.g., connectivity, expanding properties, genus, diameter, mean distance and chromatic number), partition problems (e.g., graph bisection, connectivity and separation, isoperimetric numbers, maximum cut, clustering, graph partition), and optimization problems (e.g., cutwidth, bandwidth, min-p-sum problems, ranking, scaling, quadratic assignment problem) [32–35]. We estimate the ground-truth density, namely $\rho(z)$, using the standard numerical library LAPACK [36]. This method requires a time that scales as the cube of the network size.**

NMP approximations, denoted with $\tilde{\rho}(z)$, are instead obtained **numerically solving Eqs. (9-10)**. We consider different levels of approximations. We always set $r_{\min} =$

-1 ; we consider $r_{\max} = 0$, $r_{\max} = 1$ and $r_{\max} = 2$; we vary the value of the parameter K . For $K = N \geq |N_{\max}^r|$, no heterogeneous approximation is *de facto* implemented, and the above approach reduces to the one already considered in Ref. [25].

The densities $\rho(z)$ and $\tilde{\rho}(z)$ are computed for $z \in [0, 10]$ and with a resolution $dz = 0.2$. In particular, we normalize the densities within the interval $[0, 10]$. In the NMP approximations, we use $\epsilon = 0.1$ as the value of the broadening parameter, see Ref. [25] for details. All numerical tests are performed on a server with Intel(R) Xeon(R) CPU E5-2690 v4 @ 2.60GHz CPUs and 378 GB of RAM.

Not all the networks in our corpus are part of the analysis. For $K = N$, we consider only networks with a number of nodes $N \leq 20,000$. For $K = 10$, we consider all networks with size $N \leq 100,000$. Irrespective of the level of the approximation, we let the algorithm run for up to seven days on our machine. For the slowest NMP approximation, i.e., $r_{\max} = 2$ and $K = N$, we were able to estimate the spectral density of the graph Laplacian only for 41 networks. For faster approximations, the number of analyzed networks was higher. Details are provided in Tables I–III.

We first focus our attention on how the time required for the estimation of the spectral density of the graph Laplacian using the NMP approximations scales with size of the network and the size of the largest neighborhood in the network.

Results for $K = N$ are presented in Fig. 3. The relation between computational time T^r and network size n is not very neat (Fig. 3a). However, T^r grows power like with $|N_{\max}^r|$ in a clear manner (Fig. 3b). The measured exponents are all in line with the expected complexity of the matrix inversion algorithm used to estimate messages within individual neighborhoods [25]. In fact, the inversion algorithm scales cubically with the matrix dimension, thus the computational time of the entire algorithm is dominated by the inversion of the matrix associated with the largest neighborhood in the graph.

Results for $K = 10$ are presented in Fig. 4. The relation between computational time \tilde{T}^r and network size n is clearly linear (Fig. 4a). \tilde{T}^r now grows sub-linearly with $|N_{\max}^r|$, however, the relationship is not as clear as the one that relates \tilde{T}^r to n (Fig. 4b).

In Fig. 5, we compare the ground-truth spectral density with NMP-based estimates obtained at different levels of approximation. Here, we set $r_{\min} = -1$ and $r_{\max} = 2$, and we vary K to control for the level of the approximation. The comparison is made for two real-world networks. For small K values, the approximate spectral density fails to properly capture the behavior of the ground-truth density. The accuracy greatly improves as K is increased if K is small. For sufficiently large values of K , no visible changes are apparent in the estimated densities. For example, already for $K = 10$ the approximate density appears almost identical to the one obtained for $K = N$.

We test systematically the above two observations in

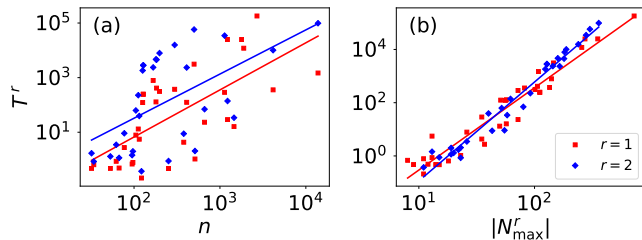


FIG. 3: **Computational time for the estimation of the spectral density of the graph Laplacian.** We consider a subset of the 109 real-world networks at our disposal. For each network, we measure the computational time T^r required by the NMP algorithm for the computation of the spectral density of the graph Laplacian. Estimates of T^r are given in seconds. **(a)** We plot T^r as a function of the network size n . The lines are power-law fits of the data points, i.e., $T^r \sim n^{\tau^r}$. Fits are obtained using simple linear regression between the log-transformed variables. We find $\tau^1 = 1.21$ (Pearson linear correlation coefficient 0.64) and $\tau^2 = 1.32(0.48)$. **(b)** We consider the same networks as in panel (a), but we test the scaling $T^r \sim |N_{\max}^r|^{\sigma^r}$. We find $\sigma^1 = 2.99(0.96)$ and $\sigma^2 = 3.56(0.98)$.

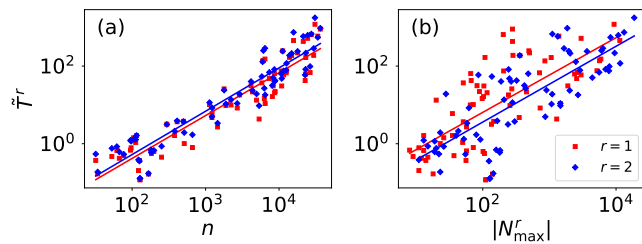


FIG. 4: **Computational time for the estimation of the spectral density of the graph Laplacian under the heterogeneous approximation.** We consider a subset of the 109 real-world networks at our disposal. For each network, we measure the computational time \tilde{T}^r required by the NMP algorithm for the computation of the spectral density of the graph Laplacian. Estimates of \tilde{T}^r are given in seconds. **(a)** We plot \tilde{T}^r as a function of the network size n . The lines are power-law fits of the data points, i.e., $\tilde{T}^r \sim n^{\tilde{\tau}^r}$. We find $\tilde{\tau}^1 = 0.98$ (Pearson linear correlation coefficient 0.93) and $\tilde{\tau}^2 = 1.00(0.94)$. **(b)** We consider the same networks as in panel (a), but we test the scaling $\tilde{T}^r \sim |N_{\max}^r|^{\tilde{\sigma}^r}$. We find $\tilde{\sigma}^1 = 0.80(0.66)$ and $\tilde{\sigma}^2 = 0.81(0.72)$.

the corpus of real networks. To compare two spectral densities, we make use of the Hellinger distance, i.e.,

$$d(\rho, \tilde{\rho}) = 1 - \int_0^{10} dz \sqrt{\rho(z)\tilde{\rho}(z)}. \quad (11)$$

By definition, we have $0 \leq d(\rho, \tilde{\rho}) \leq 1$, with $d = 0$ indicating perfect agreement between ρ and $\tilde{\rho}$. In Fig. 6a, we display the cumulative distribution of the Hellinger distance obtained over a subset of networks in our cor-

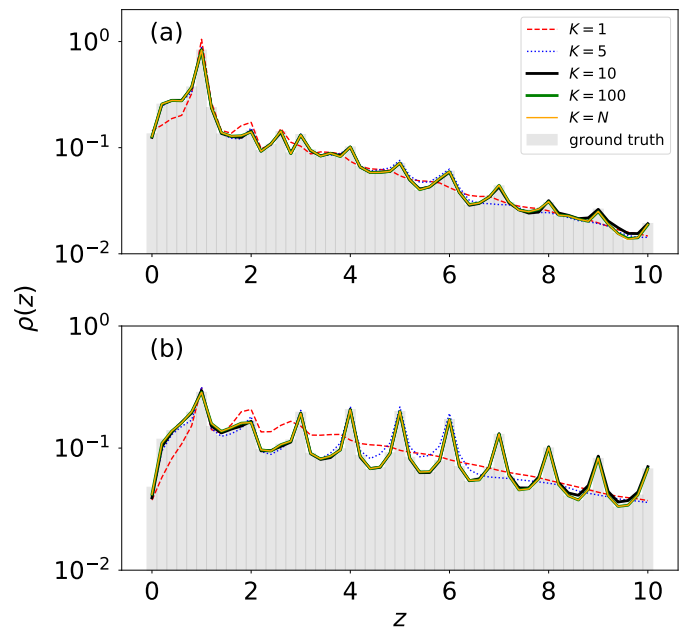


FIG. 5: **Laplacian spectral density of real-world networks.** **(a)** Spectral density of the graph Laplacian $\rho(z)$ for the network of users of the Pretty-Good-Privacy algorithm for secure information interchange [37]. The various approximations are obtained by setting $r_{\min} = -1$, $r_{\max} = 2$, but different K values. The ground-truth density is estimated using LAPACK. **(b)** Same as in panel (a), but for the Cond-Mat collaboration network [38].

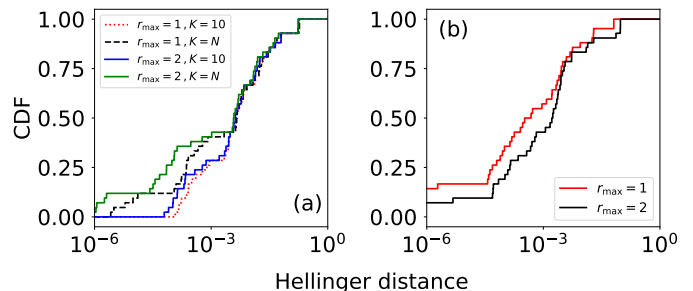


FIG. 6: **Accuracy of NMP approximations in reproducing the Laplacian spectral density of real-world networks.** **(a)** We consider a subset of the 109 real-world networks at our disposal. For each network, we estimate the Hellinger distance between the ground-truth Laplacian spectral $\rho(z)$ and its approximation $\tilde{\rho}(z)$ obtained via NMP. In all approximations, we set $r_{\min} = -1$. We vary instead the values of r_{\max} and K . For each approximation, we plot the cumulative distribution function (CDF) of the Hellinger distance over the set of analyzed networks. **(b)** For each network, we estimate the Hellinger distance between the NMP approximations obtained for $K = 10$ and $K = N$. Results of the experiments are obtained for $r_{\min} = -1$. We consider the cases $r_{\max} = 1$ and $r_{\max} = 2$.

pus. Comparisons are made between the ground-truth density and different types of approximations. All NMP-

based approximations are generally good. The accuracy of the approximation increases if we increase $r_{\max} = 1$ to $r_{\max} = 2$, and also we increase $K = 10$ to $K = N$. However, the change in accuracy is not that dramatic. Indeed, for a fixed value of r_{\max} , increasing $K = 10$ to $K = N$ generates little changes in the predicted distribution as apparent from the results of Fig. 6b. For 75% of the networks, the increase $K = 10 \rightarrow K = N$ induces a change in the predicted distribution corresponding to a value of the Hellinger distance smaller than 0.01.

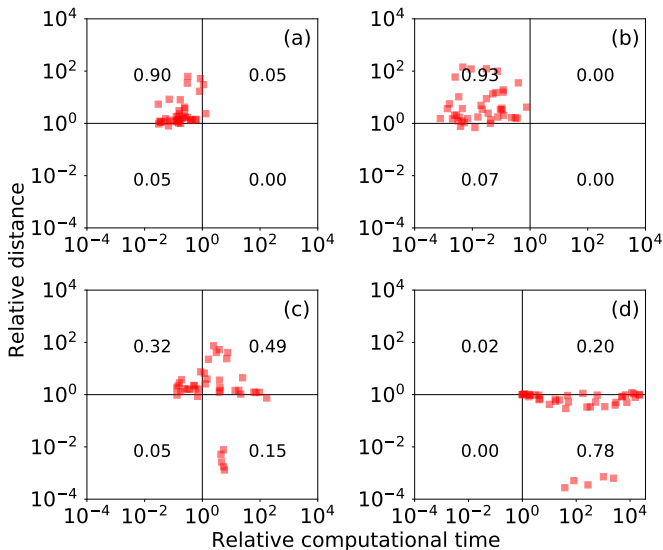


FIG. 7: **Trade off between time and accuracy in approximating the Laplacian spectral density of real-world networks.** (a) We consider the same subset of real-networks as in Fig. 6. Each point denotes a network. For each network, we estimate the Hellinger distances between the ground-truth Laplacian spectral density and two NMP approximations, namely approximations a and b , obtained for $r_{\max} = r_{\max}^{(a)} = 0$, $K = K^{(a)} = N$ and $r_{\max} = r_{\max}^{(b)} = 1$, $K = K^{(b)} = N$, respectively. We also measure the computation time required by the approximations. We then plot the ratio between the Hellinger distances of two approximations as a function of the ratio of their computational time. To facilitate the interpretation of the plot, we divided it into four quadrants. The left quadrants denote the region where approximation a is slower than approximation b ; the top quadrants indicate that approximation a is less accurate than approximation b . We also report the fraction of networks observed in each of the four quadrants. (b) Same as in (a), but for $r_{\max}^{(a)} = 0$, $K = K^{(a)} = N$ and $r_{\max}^{(b)} = 2$ and $K = K^{(b)} = N$. (c) Same as in (a), but for $r_{\max}^{(a)} = 0$, $K = K^{(a)} = N$ and $r_{\max}^{(b)} = 2$ and $K = K^{(b)} = 10$. (d) Same as in (a), but for $r_{\max}^{(a)} = 2$, $K = K^{(a)} = N$ and $r_{\max}^{(b)} = 2$ and $K = K^{(b)} = 10$.

We complete the summary of our analysis in Fig. 7. There, we compare different levels of approximations in terms of accuracy and computational time. As expected, we find that increasing r_{\max} while keeping K fixed leads to an increase of accuracy and computational

time (Figs. 7a and 7b). Only a few exceptions are visible; these are given by very small networks, with sizes $n \leq 100$. Quite surprisingly, we find that, for 49% of the analyzed networks, the proposed heterogeneous NMP approximation is faster and more accurate than the standard MP approximation (Fig. 7c). For many small networks, their performance is similar and is obtained in a similar time. The only apparent exceptions are given by five distinct snapshots of the peer-to-peer Gnutella network [39, 40], where the MP approximation greatly outperforms the NMP approximation, but with a computational time that is about two orders of magnitude larger than the NMP approximation. Finally, we confirm that the accuracy of the NMP approximation obtained for $r_{\max} = 2$ and $K = 10$ is almost identical to the one achieved for $r_{\max} = 2$ and $K = N$ (Fig. 7c). The only exceptions are still given by the five Gnutella networks. However, the greater accuracy is achieved thanks to a significant increase in computational time.

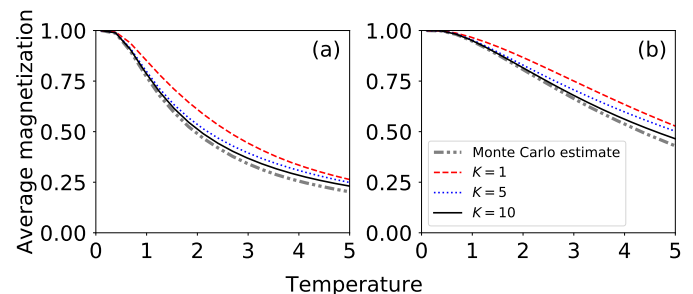


FIG. 8: **Heterogeneous belief propagation for the zero-field Ising model.** (a) Average magnetization of the zero-field Ising model for the Pretty-Good-Privacy network [37]. Results are obtained by integrating the heterogeneous NMP equations of Eqs. (4) and (5) with the belief propagation framework of [26]. The various curves are obtained by setting $r_{\min} = -1$, $r_{\max} = 2$, but allowing K to range over multiple different values. The ground-truth magnetization is estimated using the Wolff cluster MCMC algorithm. (b) Same as in panel (a), but for the Cond-Mat collaboration network [38].

V. DISCUSSION

We systematically tested the NMP approach on a corpus of 109 networks. We found, in accordance with expectations, that increasing the cycles accounted for by increasing r led to improved accuracy at the expense of speed.

We also introduced a hybrid approach, that uses more accurate approximations for low-degree nodes, and less accurate mean-field approximations at very high-degree nodes. We tested the hybrid approach in estimating the spectral density of the graph Laplacian of the real networks in our corpus. Compared to conventional MP, this approach was more accurate in 81% of networks

(Fig. 7(c): $0.49 + 0.32 = 0.81$). In addition, it was also faster in 64% of cases (Fig. 7(c): $0.49 + 0.15 = 0.64$). In a plurality of cases, the approximation was both faster and more accurate than conventional MP. The findings suggest that the NMP framework is applicable to a wide class of networks, even those with very large hubs.

The proposed NMP approach can be used in other problems whose solution can be approximated via conventional MP. Our detailed numerical experiments have focused on spectral density, a problem with ground truth that can be computed numerically for relatively large networks. However, as a final example, we consider the belief propagation framework of [26] to compute the magnetization of the zero-field Ising model. Fig. 8 shows the magnetization for $r_{\min} = -1$, $r_{\max} = 2$ and different values of K , for the same networks analyzed in Fig. 5. We see that as we increase K we get improved approximations of the magnetization, and that for $K = 10$ the results are quite close to Monte Carlo estimates.

In summary, we find that heterogeneous message passing approximations are effective for heterogeneous net-

works. Specifically, high-degree nodes can be well accounted for with conventional mean-field approaches, while the corrections due to cycles are incorporated in the lower-degree nodes. Both speed and accuracy can be simultaneously improved by applying appropriate approximations.

Acknowledgments

The authors thank Ginestra Bianconi, Christopher Moore, and Mark Newman for helpful conversations. The work was supported by National Science Foundation Grant BIGDATA-1838251 (G.T.C.), the Army Research Office Grant W911NF-21-1-0194 (F.R.), and the Air Force Office of Scientific Research Grant FA9550-21-1-0446 (F.R.). The funders had no role in study design, data collection and analysis, decision to publish, or any opinions, findings, and conclusions or recommendations expressed in the paper.

-
- [1] M. E. J. Newman, arXiv preprint arXiv:2211.05054 (2022).
 - [2] B. Karrer and M. E. J. Newman, *Physical Review E* **82**, 016101 (2010).
 - [3] A. Y. Lokhov, M. Mézard, H. Ohta, and L. Zdeborová, *Physical Review E* **90**, 012801 (2014).
 - [4] A. Y. Lokhov, M. Mézard, and L. Zdeborová, *Physical Review E* **91**, 012811 (2015).
 - [5] F. Altarelli, A. Braunstein, L. Dall’Asta, and R. Zecchina, *Journal of Statistical Mechanics: Theory and Experiment* **2013**, P09011 (2013).
 - [6] F. Altarelli, A. Braunstein, L. Dall’Asta, J. R. Wakeling, and R. Zecchina, *Physical Review X* **4**, 021024 (2014).
 - [7] G. Bianconi, H. Sun, G. Rapisardi, and A. Arenas, *Physical Review Research* **3**, L012014 (2021).
 - [8] A. Decelle, F. Krzakala, C. Moore, and L. Zdeborová, *Physical Review Letters* **107**, 065701 (2011).
 - [9] F. Radicchi, *Physical Review E* **97**, 022316 (2018).
 - [10] F. Radicchi and C. Castellano, *Physical Review Letters* **120**, 198301 (2018).
 - [11] S. N. Dorogovtsev, A. V. Goltsev, J. F. Mendes, and A. N. Samukhin, *Physical Review E* **68**, 046109 (2003).
 - [12] T. Rogers, I. P. Castillo, R. Kühn, and K. Takeda, *Physical Review E* **78**, 031116 (2008).
 - [13] B. Karrer, M. E. J. Newman, and L. Zdeborová, *Physical Review Letters* **113**, 208702 (2014).
 - [14] K. E. Hamilton and L. P. Pryadko, *Physical Review Letters* **113**, 208701 (2014).
 - [15] F. Radicchi and C. Castellano, *Nature communications* **6**, 1 (2015).
 - [16] G. Bianconi, *Physical Review E* **96**, 012302 (2017).
 - [17] G. Bianconi, *Physical Review E* **97**, 022314 (2018).
 - [18] M. Mezard and A. Montanari, *Information, Physics, and Computation* (Oxford University Press, 2009).
 - [19] D. J. C. MacKay, *Information Theory, Inference and Learning Algorithms* (Cambridge University Press, 2003).
 - [20] S. Melnik, A. Hackett, M. A. Porter, P. J. Mucha, and J. P. Gleeson, *Physical Review E* **83**, 036112 (2011).
 - [21] D. J. Watts and S. H. Strogatz, *nature* **393**, 440 (1998).
 - [22] M. E. J. Newman, *Networks* (Oxford university press, 2010).
 - [23] M. E. J. Newman, *Physical Review Letters* **103**, 058701 (2009).
 - [24] F. Radicchi and C. Castellano, *Physical Review E* **93**, 030302 (2016).
 - [25] G. T. Cantwell and M. E. J. Newman, *Proceedings of the National Academy of Sciences* **116**, 23398 (2019).
 - [26] A. Kirkley, G. T. Cantwell, and M. E. J. Newman, *Science Advances* **7**, eabf1211 (2021).
 - [27] A.-L. Barabási and R. Albert, *science* **286**, 509 (1999).
 - [28] G. Bianconi and M. Marsili, *Journal of Statistical Mechanics: Theory and Experiment* **2005**, P06005 (2005).
 - [29] F. Radicchi, *Physical Review E* **91**, 010801 (2015).
 - [30] Y. Weiss, *Neural Computation* **12**, 1–41 (2000).
 - [31] R. Zivan, O. Lev, R. Galiki, *Proceedings of the AAAI Conference on Artificial Intelligence* **34**, 7333–7340 (2020).
 - [32] R. Merris, *Linear Algebra Appl.* **197–198**, 143–176 (1994).
 - [33] F. Chung, L. Lu and V. Vu, *Proc. Natl. Acad. Sci. USA* **100**, 6313–6318 (2003).
 - [34] F. Chung, *Spectral Graph Theory* (CBMS Regional Conference Series in Mathematics, American Mathematical Society, 1997).
 - [35] T. Biyikoglu, T. Leydold and P. F. Stadler, *Laplacian Eigenvectors of Graphs: Perron–Frobenius and Faber–Krahn Type Theorems* (Lecture Notes in Mathematics, Springer, 2007).
 - [36] *LAPACK – Linear Algebra PACKage*, <https://netlib.org/lapack/>, accessed: 2023-03-28.
 - [37] M. Boguñá, R. Pastor-Satorras, A. Díaz-Guilera, and A. Arenas, *Physical Review E* **70**, 056122 (2004).
 - [38] M. E. J. Newman, *Proceedings of the National Academy*

- of Sciences **98**, 404 (2001).
- [39] M. Ripeanu, I. Foster, and A. Iamnitchi, arXiv preprint cs/0209028 (2002).
- [40] J. Leskovec, J. Kleinberg, and C. Faloutsos, ACM Transactions on Knowledge Discovery from Data (TKDD) **1**, 2 (2007).
- [41] R. Milo, S. Itzkovitz, N. Kashtan, R. Levitt, S. Shen-Orr, I. Ayzenshtat, M. Sheffer, and U. Alon, Science **303**, 1538 (2004).
- [42] W. W. Zachary, Journal of Anthropological Research pp. 452–473 (1977).
- [43] D. Lusseau, K. Schneider, O. J. Boisseau, P. Haase, E. Slooten, and S. M. Dawson, Behavioral Ecology and Sociobiology **54**, 396 (2003).
- [44] D. E. Knuth, *The Stanford GraphBase: a platform for combinatorial computing*, vol. 37 (Addison-Wesley Reading, 1993).
- [45] S. Mangan and U. Alon, Proceedings of the National Academy of Sciences **100**, 11980 (2003).
- [46] L. A. Adamic and N. Glance, in *Proceedings of the 3rd international workshop on Link discovery* (ACM, 2005), pp. 36–43.
- [47] M. E. J. Newman, Physical Review E **74**, 036104 (2006).
- [48] M. Girvan and M. E. J. Newman, Proceedings of the National Academy of Sciences **99**, 7821 (2002).
- [49] J. Fournet and A. Barrat, PloS one **9**, e107878 (2014).
- [50] R. Ulanowicz, C. Bondavalli, and M. Egnotovich, Annual Report to the United States Geological Service Biological Resources Division Ref. No.[UMCES] CBL pp. 98–123 (1998).
- [51] J. Kunegis, in *Proc. Int. Conf. on World Wide Web Companion* (2013), pp. 1343–1350, URL <http://userpages.uni-koblenz.de/~kunegis/paper/kunegis-koblenz-network-collection.pdf>.
- [52] R. Michalski, S. Palus, and P. Kazienko, in *Lecture Notes in Business Information Processing* (Springer Berlin Heidelberg, 2011), vol. 87, pp. 197–206.
- [53] N. D. Martinez, Ecological Monographs pp. 367–392 (1991).
- [54] P. M. Gleiser and L. Danon, Advances in complex systems **6**, 565 (2003).
- [55] L. Isella, J. Stehlé, A. Barrat, C. Cattuto, J.-F. Pinton, and W. Van den Broeck, Journal of theoretical biology **271**, 166 (2011).
- [56] V. Colizza, R. Pastor-Satorras, and A. Vespignani, Nature Physics **3**, 276 (2007).
- [57] R. Milo, S. Shen-Orr, S. Itzkovitz, N. Kashtan, D. Chklovskii, and U. Alon, Science **298**, 824 (2002).
- [58] R. Guimera, L. Danon, A. Diaz-Guilera, F. Giralt, and A. Arenas, Physical Review E **68**, 065103 (2003).
- [59] H. Jeong, S. P. Mason, A.-L. Barabási, and Z. N. Oltvai, Nature **411**, 41 (2001).
- [60] T. Opsahl and P. Panzarasa, Social networks **31**, 155 (2009).
- [61] D. Bu, Y. Zhao, L. Cai, H. Xue, X. Zhu, H. Lu, J. Zhang, S. Sun, L. Ling, N. Zhang, et al., Nucleic acids research **31**, 2443 (2003).
- [62] T. Opsahl, F. Agneessens, and J. Skvoretz, Social Networks **32**, 245 (2010).
- [63] F. Radicchi, PloS one **6**, e17249 (2011).
- [64] G. Joshi-Tope, M. Gillespie, I. Vastrik, P. D’Eustachio, E. Schmidt, B. de Bono, B. Jassal, G. Gopinath, G. Wu, L. Matthews, et al., Nucleic acids research **33**, D428 (2005).
- [65] L. Šubelj and M. Bajec, in *Proceedings of the First International Workshop on Software Mining* (ACM, 2012), pp. 9–16.
- [66] J. Leskovec, J. Kleinberg, and C. Faloutsos, in *Proceedings of the eleventh ACM SIGKDD international conference on Knowledge discovery in data mining* (ACM, 2005), pp. 177–187.
- [67] M. Ley, in *String Processing and Information Retrieval* (Springer, 2002), pp. 1–10.
- [68] G. Palla, I. J. Farkas, P. Pollner, I. Derényi, and T. Vicsek, New Journal of Physics **9**, 186 (2007).
- [69] G. R. Kiss, C. Armstrong, R. Milroy, and J. Piper, The computer and literary studies pp. 153–165 (1973).
- [70] L. Šubelj and M. Bajec, in *Proceedings of the 22nd international conference on World Wide Web companion* (International World Wide Web Conferences Steering Committee, 2013), pp. 527–530.
- [71] M. De Choudhury, H. Sundaram, A. John, and D. D. Seligmann, in *Computational Science and Engineering, 2009. CSE’09. International Conference on* (IEEE, 2009), vol. 4, pp. 151–158.
- [72] J. Leskovec, K. J. Lang, A. Dasgupta, and M. W. Mahoney, Internet Mathematics **6**, 29 (2009).
- [73] V. Gómez, A. Kaltenbrunner, and V. López, in *Proceedings of the 17th international conference on World Wide Web* (ACM, 2008), pp. 645–654.
- [74] B. Viswanath, A. Mislove, M. Cha, and K. P. Gummadi, in *Proceedings of the 2nd ACM workshop on Online social networks* (ACM, 2009), pp. 37–42.
- [75] M. Richardson, R. Agrawal, and P. Domingos, in *The Semantic Web-ISWC 2003* (Springer, 2003), pp. 351–368.
- [76] J. Kunegis, A. Lommatzsch, and C. Bauchhage, in *Proceedings of the 18th international conference on World wide web* (ACM, 2009), pp. 741–750.
- [77] J. McAuley and J. Leskovec, in *Advances in Neural Information Processing Systems* (2012), pp. 548–556.
- [78] U. Brandes and J. Lerner, Journal of classification **27**, 279 (2010).
- [79] E. Cho, S. A. Myers, and J. Leskovec, in *Proceedings of the 17th ACM SIGKDD international conference on Knowledge discovery and data mining* (ACM, 2011), pp. 1082–1090.
- [80] L. Brozovsky and V. Petricek, arXiv preprint cs/0703042 (2007).
- [81] J. Kunegis, G. Gröner, and T. Gotttron, in *Proceedings of the 4th ACM RecSys workshop on Recommender systems and the social web* (ACM, 2012), pp. 37–44.
- [82] J. Leskovec, L. A. Adamic, and B. A. Huberman, ACM Transactions on the Web (TWEB) **1**, 5 (2007).
- [83] R. Albert, H. Jeong, and A.-L. Barabási, Nature **401**, 130 (1999).
- [84] G. Palla, I. J. Farkas, P. Pollner, I. Derényi, and T. Vicsek, New Journal of Physics **10**, 123026 (2008).
- [85] K. D. Bollacker, S. Lawrence, and C. L. Giles, in *Proceedings of the second international conference on Autonomous agents* (ACM, 1998), pp. 116–123.
- [86] X. Niu, X. Sun, H. Wang, S. Rong, G. Qi, and Y. Yu, in *The Semantic Web-ISWC 2011* (Springer, 2011), pp. 205–220.
- [87] J. Yang and J. Leskovec, in *Proceedings of the ACM SIGKDD Workshop on Mining Data Semantics* (ACM, 2012), p. 3.
- [88] B. H. Hall, A. B. Jaffe, and M. Trajtenberg, Tech. Rep.,

National Bureau of Economic Research (2001).

- [89] S. Auer, C. Bizer, G. Kobilarov, J. Lehmann, R. Cyganik, and Z. Ives, *Dbpedia: A nucleus for a web of open data* (Springer, 2007).
- [90] A. Mislove, M. Marcon, K. P. Gummadi, P. Druschel, and B. Bhattacharjee, in *Proceedings of the 7th ACM SIGCOMM conference on Internet measurement* (ACM, 2007), pp. 29–42.

Network	Ref.	URL	N	E	$ N_{\max}^1 $	$ N_{\max}^2 $	T^1	T^2	\tilde{T}^1	\tilde{T}^2
*Social 3	[41]	url	32	80	14	22	0	1	0	0
*Karate club	[42]	url	34	78	18	23	0	0	0	0
*Protein 2	[41]	url	53	123	8	19	0	1	0	0
*Dolphins	[43]	url	62	159	12	26	0	3	0	0
*Social 1	[41]	url	67	142	11	18	0	1	0	0
*Les Miserables	[44]	url	77	254	36	55	2	9	0	0
*Protein 1	[41]	url	95	213	7	12	0	1	0	1
*E. Coli, transcription	[45]	url	97	212	11	18	0	1	0	1
*Political books	[46]	url	105	441	25	51	7	62	1	1
*David Copperfield	[47]	url	112	425	50	92	13	227	1	1
*College football	[48]	url	115	613	13	39	5	39	1	1
*S 208	[41]	url	122	189	10	10	0	0	0	0
*High school, 2011	[49]	url	126	1,709	56	124	122	1,824	0	0
*Bay Dry	[50, 51]	url	128	2,106	111	128	244	2,801	0	0
*Bay Wet	[51]	url	128	2,075	111	128	248	2,858	0	0
*Radoslaw Email	[51, 52]	url	167	3,250	139	143	791	2,371	0	0
*High school, 2012	[49]	url	180	2,220	56	158	129	4,681	0	0
*Little Rock Lake	[51, 53]	url	183	2,434	105	180	413	4,526	0	0
*Jazz	[54]	url	198	2,742	101	182	313	7,915	0	0
*S 420	[41]	url	252	399	15	14	0	0	0	0
*C. Elegans, neural	[21]	url	297	2,148	134	239	374	15,720	3	3
*Network Science	[47]	url	379	914	35	42	4	8	1	2
*Dublin	[51, 55]	url	410	2,765	50	164	124	2,342	3	3
*US Air Trasportation	[56]	url	500	2,980	146	301	3,119	57,958	3	3
*S 838	[41]	url	512	819	23	23	1	2	1	1
*Yeast, transcription	[57]	url	662	1,062	72	80	23	69	0	1
*URV email	[58]	url	1,133	5,451	72	279	289	34,546	10	11
Political blogs	[46]	url	1,222	16,714	351	867	24,944	–	4	4
*Air traffic	[51]	url	1,226	2,408	35	62	28	139	5	8
*Yeast, protein	[59]	url	1,458	1,948	57	57	16	34	2	3
Petster, hamster	[51]	url	1,788	12,476	272	904	24,879	–	25	23
UC Irvine	[51, 60]	url	1,893	13,835	256	1,076	11,963	–	9	10
Yeast, protein	[61]	url	2,224	6,609	65	208	–	–	9	13
Japanese	[41]	url	2,698	7,995	726	1,459	181,172	–	8	10
Open flights	[51, 62]	url	2,905	15,645	242	1,101	–	–	18	18
*GR-QC, 1993-2003	[40]	url	4,158	13,422	81	187	356	10,098	31	40
Tennis	[63]	url	4,338	81,865	452	2,015	–	–	21	23

TABLE I: From left to right, we report: the name of the network, the reference of the paper(s) where the network was first analyzed, the URL where the network was retrieved, the number of nodes and edges of the network, the number of nodes in the largest neighborhoods of orders $r = 1$ and $r = 2$, and the computational time needed to obtain the spectral density of the graph Laplacian via the NMP approximation with $r_{\max} = 1$ and $K = N$, $r_{\max} = 2$ and $K = N$, $r_{\max} = 1$ and $K = 10$, and $r_{\max} = 2$ and $K = 10$. The analysis was performed on the largest connected component of each network. Computational time is measured in seconds, and the reported value is rounded to the nearest integer. A computational time equal to zero seconds means that less than 0.5 seconds were required to estimate the spectral density of the graph Laplacian. No computational time is reported for networks that could not be analyzed due to their high computational demand. The asterisk before the network name indicate that we were able to fully compute their spectrum, either exactly or using the various NMP approximations. These are the only networks included in the analysis of Figs. 6 and 7.

Network	Ref.	URL	N	E	N_{\max}^1	N_{\max}^2	T^1	T^2	\tilde{T}^1	\tilde{T}^2
US Power grid	[21]	url	4,941	6,594	20	28	—	—	13	19
HT09	[55]	url	5,352	18,481	1,288	1,464	—	—	4	9
Hep-Th, 1995-1999	[38]	url	5,835	13,815	50	136	—	—	36	53
Reactome	[51, 64]	url	5,973	145,778	855	2,492	—	—	135	129
Jung	[51, 65]	url	6,120	50,290	5,656	6,050	—	—	137	250
Gnutella, Aug. 8, 2002	[39, 40]	url	6,299	20,776	98	440	—	—	14	26
JDK	[51]	url	6,434	53,658	5,923	6,356	—	—	151	288
AS Oregon	[66]	url	6,474	12,572	1,459	2,685	—	—	10	18
English	[41]	url	7,377	44,205	2,569	5,585	—	—	47	69
Gnutella, Aug. 9, 2002	[39, 40]	url	8,104	26,008	103	421	—	—	16	31
French	[41]	url	8,308	23,832	1,892	4,405	—	—	30	50
Hep-Th, 1993-2003	[40]	url	8,638	24,806	65	244	—	—	64	82
Gnutella, Aug. 6, 2002	[39, 40]	url	8,717	31,525	115	266	—	—	20	40
Gnutella, Aug. 5, 2002	[39, 40]	url	8,842	31,837	89	321	—	—	22	42
PGP	[37]	url	10,680	24,316	206	481	—	—	74	63
Gnutella, August 4 2002	[39, 40]	url	10,876	39,994	103	250	—	—	30	47
Hep-Ph, 1993-2003	[40]	url	11,204	117,619	491	1,960	—	—	247	242
Spanish	[41]	url	11,558	43,050	2,986	7,814	—	—	59	75
DBLP, citations	[51, 67]	url	12,495	49,563	710	2,876	—	—	67	77
Spanish	[51]	url	12,643	55,019	5,170	11,524	—	—	75	117
*Cond-Mat, 1995-1999	[38]	url	13,861	44,619	107	358	1,478	98,257	167	188
Astrophysics	[38]	url	14,845	119,652	361	2,050	—	—	187	212
Google	[68]	url	15,763	148,585	11,401	13,208	—	—	455	740
AstroPhys, 1993-2003	[40]	url	17,903	196,972	504	3,661	—	—	219	240
Cond-Mat, 1993-2003	[40]	url	21,363	91,286	280	1,335	—	—	433	582
Gnutella, Aug. 25, 2002	[39, 40]	url	22,663	54,693	67	85	—	—	42	59
Internet	-	url	22,963	48,436	2,390	6,954	—	—	62	82
Thesaurus	[51, 69]	url	23,132	297,094	1,062	9,528	—	—	165	217
Cora	[51, 70]	url	23,166	89,157	377	818	—	—	—	—
Linux, mailing list	[51]	url	24,567	158,164	2,989	10,805	—	—	520	622
AS Caida	[66]	url	26,475	53,381	2,629	7,940	—	—	68	97
Gnutella, Aug. 24, 2002	[39, 40]	url	26,498	65,359	355	860	—	—	—	—
Hep-Th, citations	[40, 51]	url	27,400	352,021	2,469	9,467	—	—	—	—
Cond-Mat, 1995-2003	[38]	url	27,519	116,181	202	1,108	—	—	648	672
Digg	[51, 71]	url	29,652	84,781	283	1,657	—	—	189	286
Linux, soft.	[51]	url	30,817	213,208	9,339	18,740	—	—	1,195	1,759
Enron	[72]	url	33,696	180,811	1,383	8,264	—	—	590	550

TABLE II: Continuation of Table I.

Network	Ref.	URL	N	E	$ N_{\max}^1 $	$ N_{\max}^2 $	T^1	T^2	\tilde{T}^1	\tilde{T}^2
Hep-Ph, citations	[40, 51]	url	34,401	420,784	846	4,440	—	—	—	—
Cond-Mat, 1995-2005	[38]	url	36,458	171,735	278	1,855	—	—	899	948
Gnutella, Aug. 30, 2002	[39, 40]	url	36,646	88,303	56	86	—	—	—	—
Slashdot	[51, 73]	url	51,083	116,573	2,916	7,732	—	—	—	—
Gnutella, Aug. 31, 2002	[39, 40]	url	62,561	147,878	96	111	—	—	—	—
Facebook	[74]	url	63,392	816,886	1,099	14,291	—	—	—	—
Epinions	[51, 75]	url	75,877	405,739	3,045	16,661	—	—	—	—
Slashdot zoo	[51, 76]	url	79,116	467,731	2,534	16,810	—	—	—	—
Flickr	[51, 77]	url	105,722	2,316,668	5,425	15,360	—	—	—	—
Wikipedia, edits	[51, 78]	url	113,123	2,025,910	20,153	72,317	—	—	—	—
Petster, cats	[51]	url	148,826	5,447,464	80,634	136,538	—	—	—	—
Gowalla	[51, 79]	url	196,591	950,327	14,730	55,087	—	—	—	—
Libimseti	[51, 80, 81]	url	220,970	17,233,144	33,390	181,596	—	—	—	—
EU email	[40, 51]	url	224,832	339,925	7,636	20,391	—	—	—	—
Web Stanford	[72]	url	255,265	1,941,926	38,625	54,427	—	—	—	—
Amazon, Mar. 2, 2003	[82]	url	262,111	899,792	420	944	—	—	—	—
DBLP, collaborations	[51, 67]	url	317,080	1,049,866	344	1,431	—	—	—	—
Web Notre Dame	[83]	url	325,729	1,090,108	10,722	17,682	—	—	—	—
MathSciNet	[84]	url	332,689	820,644	496	2,454	—	—	—	—
CiteSeer	[51, 85]	url	365,154	1,721,981	1,739	5,392	—	—	—	—
Zhishi	[51, 86]	url	372,840	2,318,025	127,067	128,431	—	—	—	—
Actor coll. net.	[27, 51]	url	374,511	15,014,839	3,956	125,645	—	—	—	—
Amazon, Mar. 12, 2003	[82]	url	400,727	2,349,869	2,747	6,158	—	—	—	—
Amazon, Jun. 6, 2003	[82]	url	403,364	2,443,311	2,752	5,738	—	—	—	—
Amazon, May 5, 2003	[82]	url	410,236	2,439,437	2,760	6,491	—	—	—	—
Petster, dogs	[51]	url	426,485	8,543,321	46,504	313,475	—	—	—	—
Road network PA	[72]	url	1,087,562	1,541,514	9	13	—	—	—	—
YouTube friend. net.	[51, 87]	url	1,134,890	2,987,624	28,755	137,387	—	—	—	—
Road network TX	[72]	url	1,351,137	1,879,201	13	19	—	—	—	—
AS Skitter	[66]	url	1,694,616	11,094,209	35,455	128,203	—	—	—	—
Road network CA	[72]	url	1,957,027	2,760,388	13	17	—	—	—	—
Wikipedia, pages	[84]	url	2,070,367	42,336,614	230,041	1,640,275	—	—	—	—
US Patents	[51, 88]	url	3,764,117	16,511,740	794	4,228	—	—	—	—
DBpedia	[51, 89]	url	3,915,921	12,577,253	469,692	897,744	—	—	—	—
LiveJournal	[51, 90]	url	5,189,809	48,688,097	15,018	182,439	—	—	—	—

TABLE III: Continuation of Tables I and II.